Supporting Information

Goldstein et al. 10.1073/pnas.1306160110

SI Experimental Procedures

Antibodies. Antibodies used for immunoblotting were β-actin (C4; Chemicon), ataxia telangiectasia mutated (ATM) kinase (MAT3; gift from Y. Shiloh, Tel-Aviv University, Israel), pKAP1 S824 (Bethyl Laboratories), HA (HA.11; Covance), pCHK2 T68 (Cell Signaling), pATM S1981 (Epitomics), pATM S1987 (1), nucleolin (MS-3; Santa Cruz, and ab70493; Abcam), and GFP (ab1218, Abcam).

ChIP. ChIP experiments and I-PpoI site breakage/repair assays were performed as previously described (2, 3). In addition, the ChIP protocol was adapted for use with magnetic beads (Dynabeads M-280 Sheep anti-Mouse or Dynabeads M-280 Sheep anti-Rabbit; Invitrogen) for increased efficiency and specificity of immunoprecipitations. Cells expressing ddI-PpoI were treated with Shield-1 for 3 h followed by 4-hydroxytestosterone (4-OHT) and were collected for ChIP at indicated time points after cross-linking proteins and DNA by 1% formaldehyde. Immunoprecipitations were washed first in low-salt wash (150 mM NaCl, 0.1% SDS, 1% Triton X-100, 2 mM EDTA, 20 mM Tris·HCl), followed by high-salt wash (500 mM NaCl, 0.1% SDS, 1% Triton X-100, 2 mM EDTA, 20 mM Tris·HCl), followed by three washes in LiCl wash [0.25 M LiCl, 1% octylphenoxypolyethoxyethanol (IGEPAL; Sigma-Aldrich), 1% deoxycholic acid, 1% IGEPAL, 10 mM Tris·HCl]. Washes were performed by rotation at room temperature for 5 min. Samples were collected on magnetic separation racks during washes (Qiagen). Samples were eluted and prepared as previously described (2, 3). Primer sequences for the real-time PCR are listed in Table S1. Input DNA was used as an internal control for each quantitative PCR (qPCR). Antibodies used for the ChIP assay were normal rabbit IgG (Cell Signaling), ATM (Calbiochem), pNBS1 (Ser343; Cell Signaling), histone H2A (ab18255; Abcam), histone H2B (ab1790; Abcam), histone H3 (Millipore), histone 4 (H4) (Millipore), XRCC4 (ab145; Abcam), nucleolin (ab70493;), NBS1 (NB100-143; Novus), RAD50 (ab3622; Abcam), RPA32 (ab61184; Abcam), and GFP (ab290l; Abcam). Relative occupancy was calculated with threshold cycle (Ct) values normalized to input as internal control. Appropriate negative controls using normal rabbit IgG were performed for all ChIP experiments. For all ChIP experiments data are shown as mean ± SEM of two independent experiments. The *y*-axis in figures displaying ChIP results shows the relative occupancy normalized to the untreated control. *P* value was calculated for the site 182 bp 3′ or 407 bp 5′ of the double-stranded break (DSB).

DSB-Repair Assay. Serum-starved cells expressing ddI-PpoI were treated with Shield-1 for 3 h followed by a 15-min pulse of 4-OHT in the presence of Shield-1 and then were washed and allowed to recover. At indicated time points cells were washed with PBS, and lysis buffer [50 mM Tris·HCl (pH 7.5), 150 mM NaCl, 1% IGEPAL, 0.5% sodium deoxycholate, 10 mM $MgSO_4$, 1 mM DTT, 1 mg/mL RNase A, 500 U/mL HaeIII) was added followed by 30-min incubation at 37 °C. Proteinase K was added for 5 min at 37 °C, and samples were collected and stored at −80 °C. Samples were eluted and prepared as previously described (2, 3). Primer sequences for the real-time PCR are listed in Table S1. To quantify the DSBs, qPCR was performed using primers that flank the I-PpoI cut site, and the Ct values were normalized to Ct values from qPCR for GAPDH for each sample using the ΔΔCt method. For all DSB repair experiments data are shown as mean ± SEM of three independent experiments.

Cell-Death Analysis. Cell death was an analyzed by quantification of the sub-G1 subpopulation as described elsewhere (4). Clonogenic assays were performed as described elsewhere (5). For all experiments analyzing cell death, data are shown as mean ± SEM of three independent experiments.

Immunofluorescence Microscopy. Immunostaining of DNA damage-induced foci was performed as described elsewhere (6). The primary antibody used was anti–phospho-H2AX (Ser139) (Clone JBW301; Millipore). Data are shown as the mean ± SEM of three independent experiments.

Protein Coimmunoprecipitation. At indicated time points cells were treated with 1% formaldehyde for 10 min followed by glycine to terminate the reaction or were harvested without protein cross-linking. Cells were washed with PBS and lysed on ice in TGN buffer [50 mM Tris (pH 7.5), 200 mM NaCl, 50 mM NaF, protease inhibitors] for 30 min followed by sonication if proteins were cross-linked. Samples were precleared with Protein A/Protein G agarose beads (Calbiochem) and were incubated with the indicated antibodies or with normal rabbit IgG and Protein A/Protein G agarose beads overnight, washed with TGN buffer, and analyzed by immunoblot. Antibodies used were nucleolin (ab70493; Abcam), NBS1 (NB100-143; Novus), RAD50 (ab3622; Abcam), and MRE11 (NB100-142; Novus).

Statistical Analysis. Data were analyzed by the Student's *t*-test to determine the *P* value.

1. Valentin-Vega YA, et al. (2012) Mitochondrial dysfunction in ataxia-telangiectasia. *Blood* 119(6):1490–1500.
2. Berkovich E, Monnat RJ, Jr., Kastan MB (2007) Roles of ATM and NBS1 in chromatin structure modulation and DNA double-strand break repair. *Nat Cell Biol* 9(6): 683–690.
3. Berkovich E, Monnat RJ, Jr., Kastan MB (2008) Assessment of protein dynamics and DNA repair following generation of DNA double-strand breaks at defined genomic sites. *Nat Protoc* 3(5):915–922.
4. Roos W, Baumgartner M, Kaina B (2004) Apoptosis triggered by DNA damage O6-methylguanine in human lymphocytes requires DNA replication and is mediated by p53 and Fas/CD95/Apo-1. *Oncogene* 23(2):359–367.
5. Rainey MD, Charlton ME, Stanton RV, Kastan MB (2008) Transient inhibition of ATM kinase is sufficient to enhance cellular sensitivity to ionizing radiation. *Cancer Res* 68(18):7466–7474.
6. Kitagawa R, Bakkenist CJ, McKinnon PJ, Kastan MB (2004) Phosphorylation of SMC1 is a critical downstream event in the ATM-NBS1-BRCA1 pathway. *Genes Dev* 18(12):1423–1438.

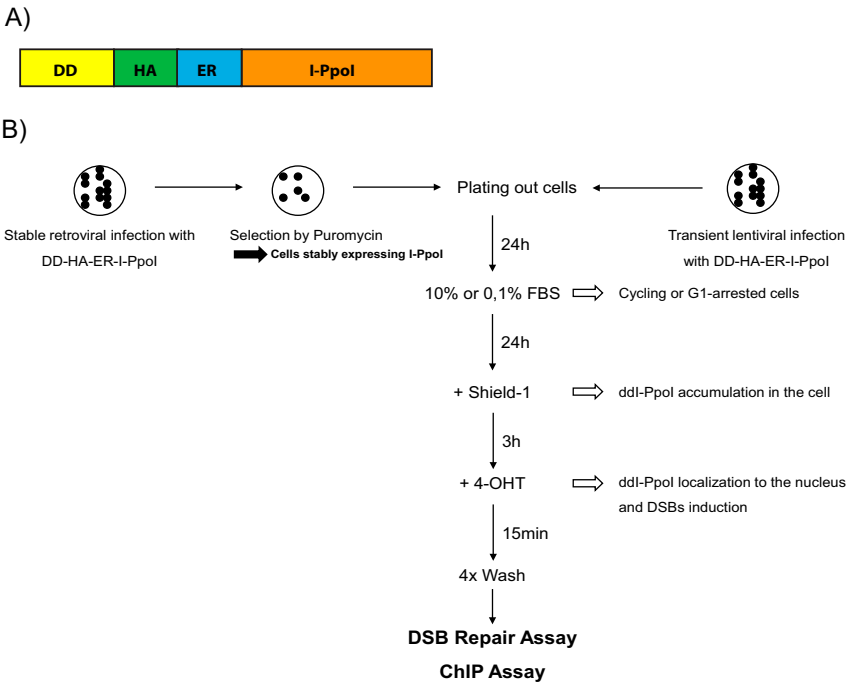

Fig. S1. The ddI-PpoI system. (*A*) A schematic diagram displaying the domains of the ddI-PpoI fusion protein that was used in this study. DD, destabilization domain; HA, hemagglutinin; ER, estrogen receptor. (*B*) A schematic description of the experimental procedure using the ddI-PpoI system to monitor DSB repair and protein dynamics at the DSB.

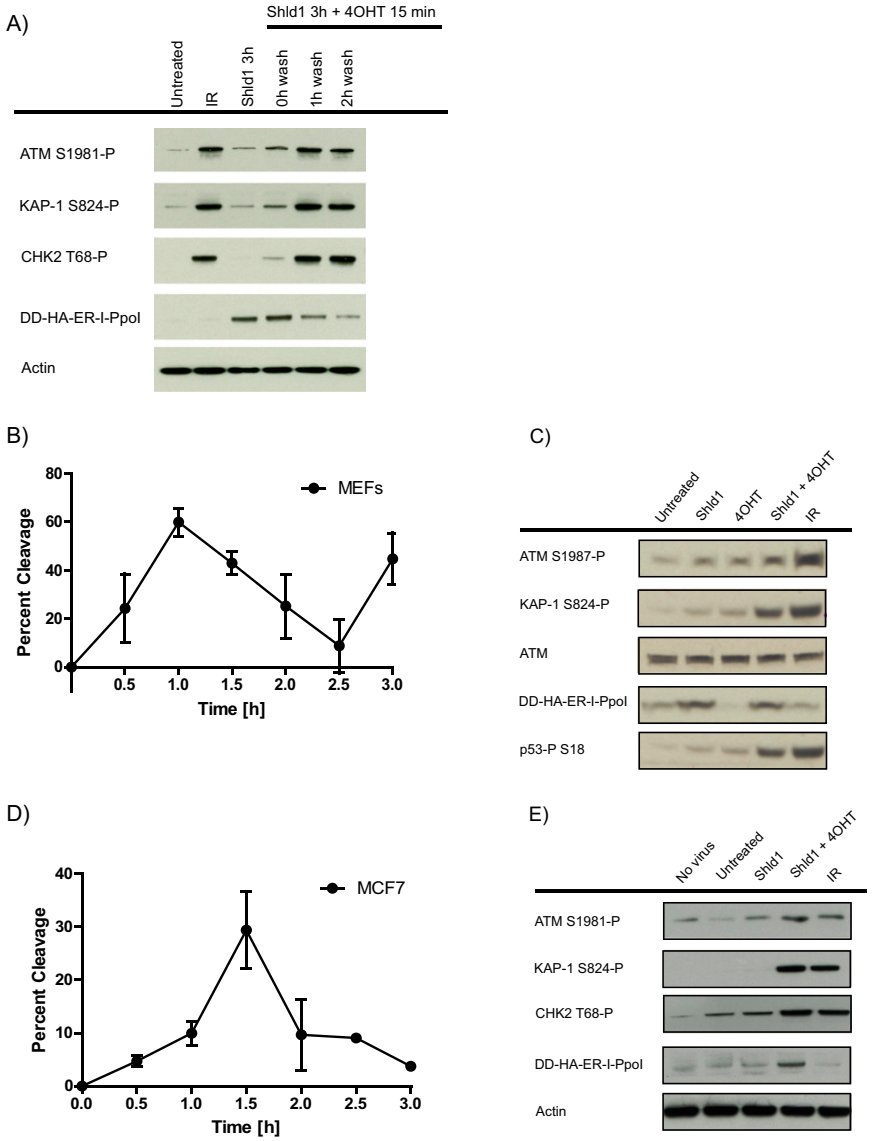

Fig. S2. Induction of ddI-PpoI activates ATM-dependent DNA-damage response (DDR) pathway. (*A*) Western blot showing the activation of the ATM-dependent DDR pathway and ddI-PpoI expression after ddI-PpoI induction or 30 min after 1-Gy ionizing radiation (IR) in MCF7 cells. MCF7 cells stably expressing ddI-PpoI were treated with Shield-1 for 3 h followed by 4-OHT for 15 min and were washed and harvested at the indicated time points. Whole-cell extracts were used for immunoblotting. (*B*) DNA-repair assay in $Arf^{-/-}$ mouse embryonic fibroblasts (MEFs) transiently transduced with a retroviral cassette expressing ddI-PpoI as described in Fig. 1*A*. (*C*) Western Blot as described in *A* in $Arf^{-/-}$ MEFs transiently transduced with a retroviral cassette expressing ddI-PpoI. (*D*) DNA-repair assay in MCF7 cells transiently transduced with a lentiviral cassette expressing ddI-PpoI as described in Fig. 1*A*. (*E*) Western blot as described in *A* in MCF7 cells transiently transduced with a lentiviral cassette expressing ddI-PpoI.

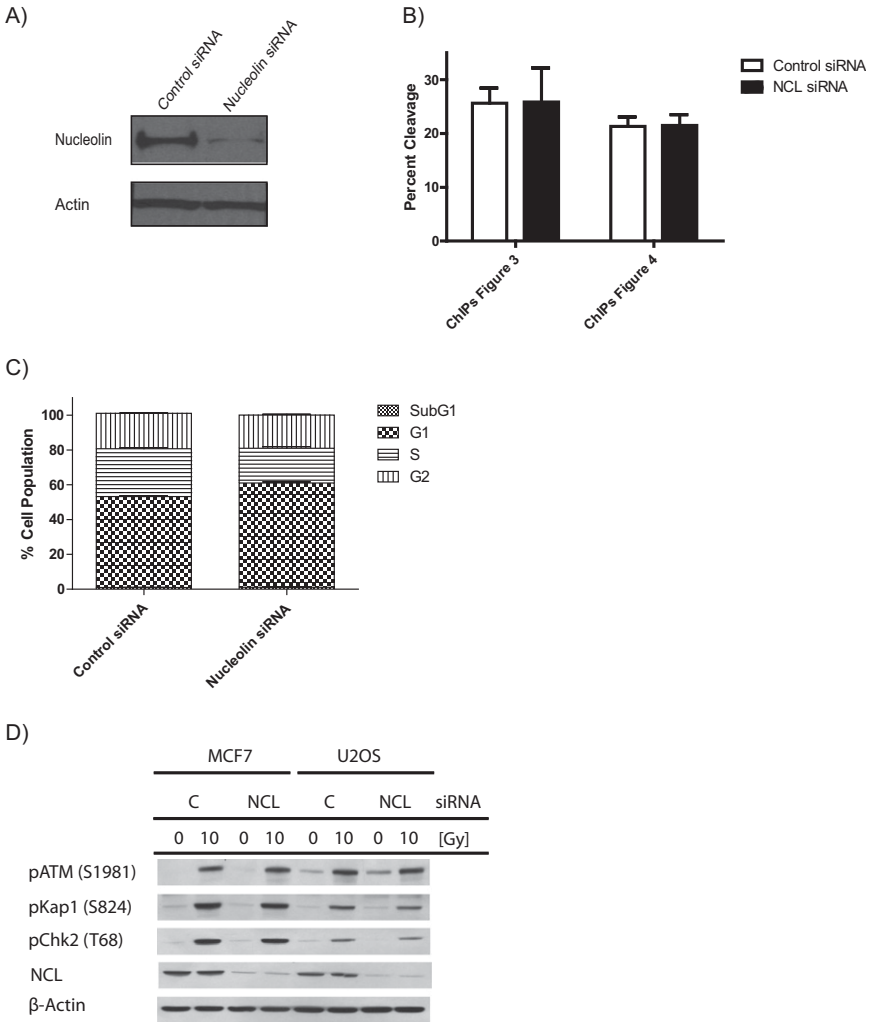

Fig. S3. Nucleolin knockdown does not affect DSB induction by ddI-PpoI, cell-cycle progression, or DDR. (*A*) Western blot showing down-regulation of nucleolin expression by siRNA. (*B*) DNA-repair assay as described in Fig. 1*A* used to determine the DNA cleavage at the chromosome 1 site 1 h after ddI-PpoI induction using input DNA from ChIP assays shown in Figs. 3 and 4 *C* and *D*. Each bar shows the mean of two independent ChIP experiments ± SEM. (*C*) Quantification of cell populations in the SubG1, G1, S, and G2 phases of the cell cycle by PI staining in MCF7 cells 72 h after transfection with nontargeting control siRNA or nucleolin-targeting siRNA. Data are shown as the mean ± SEM of three independent experiments. (*D*) Western blot showing the activation of the ATM-dependent DDR signaling pathway in MCF7 and U2OS cells 30 min after 10 Gy ionizing radiation. Cells were transfected with control or nucleolin-targeting siRNA.

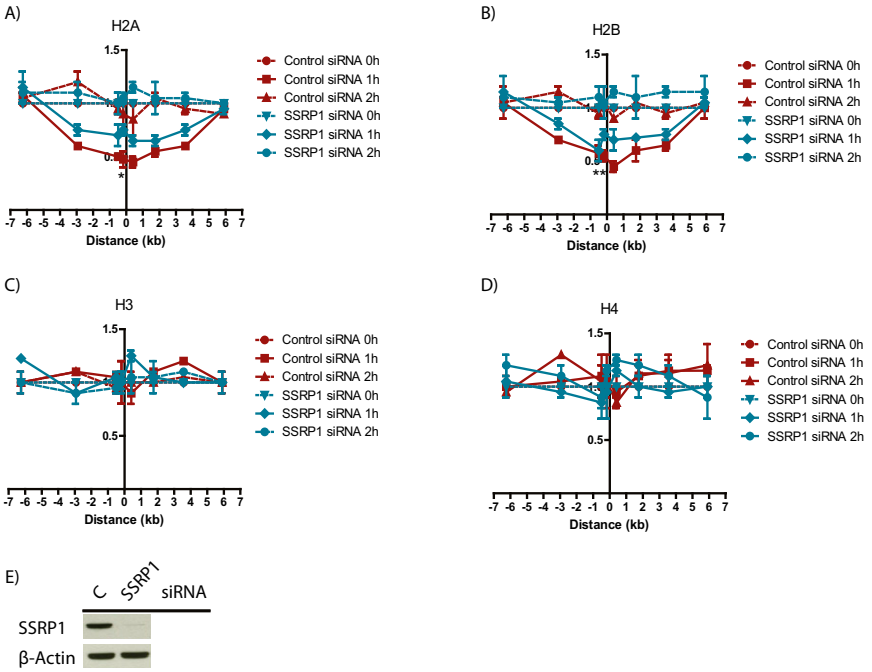

Fig. S4. Knockdown of the FACT complex subunit structure-specific recognition protein 1 (SSRP1) marginally affects nucleosome disruption. ChIP of (*A*) histone H2A, (*B*) histone H2B, (*C*) histone H3, and (*D*) histone H4 in MCF7 cells stably expressing ddI-PpoI as described in Fig. 1*B* that were cultivated in medium containing 0.1% FBS for 24 h before DSB induction. Cells were transfected with nontargeting control siRNA or SSRP1-targeting siRNA. (*E*) Western blot showing down-regulation of SSRP1 expression by siRNA. $*P = 0.093$, $**P = 0.106$.

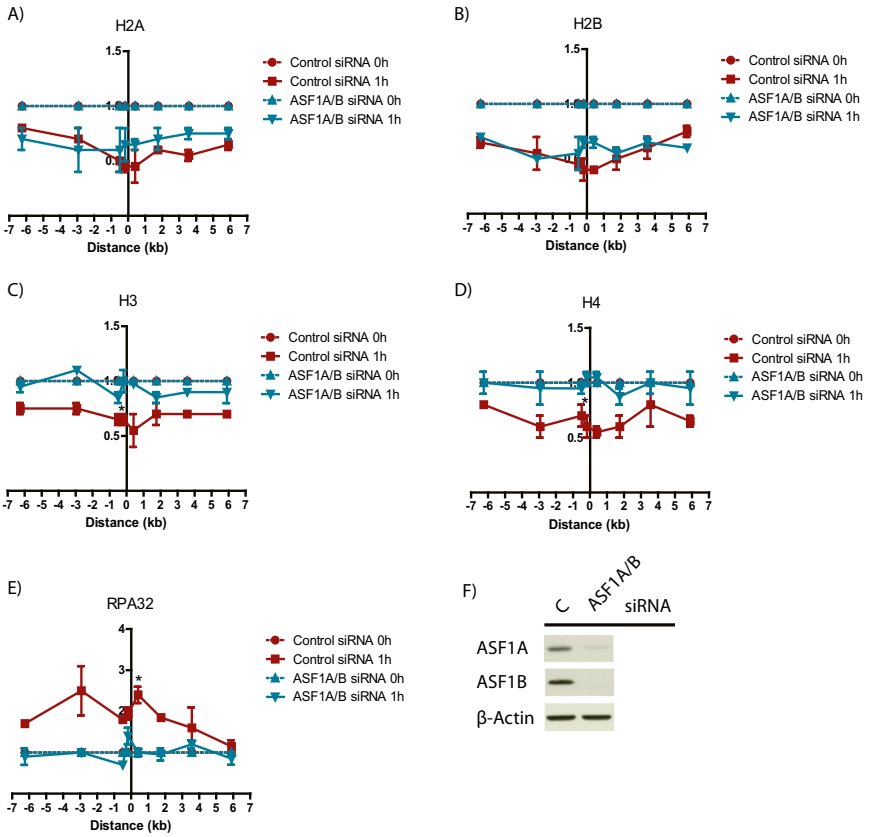

Fig. S5. Anti-silencing function 1 A and B (ASF1A/B) activity is involved in the removal of the H3/H4 histone dimer during nucleosome disruption. (*A–D*) Simultaneous knockdown of ASF1A and ASF1B attenuates the eviction of H3 and H4 and RPA recruitment to the DSB in cycling cells. ChIP of (*A*) histone H2A, (*B*) histone H2B, (*C*) histone H3, (*D*) histone H4, and (*E*) RPA32 in MCF7 cells stably expressing ddI-PpoI as described in Fig. 1*B* that were cultivated in medium containing 10% FBS for 24 h before DSB induction. Cells were transfected with nontargeting control siRNA or ASF1A- and ASF1B-targeting siRNA. (*F*) Western blot showing down-regulation of ASF1A and ASF1B expression by siRNA. $*P < 0.05$.

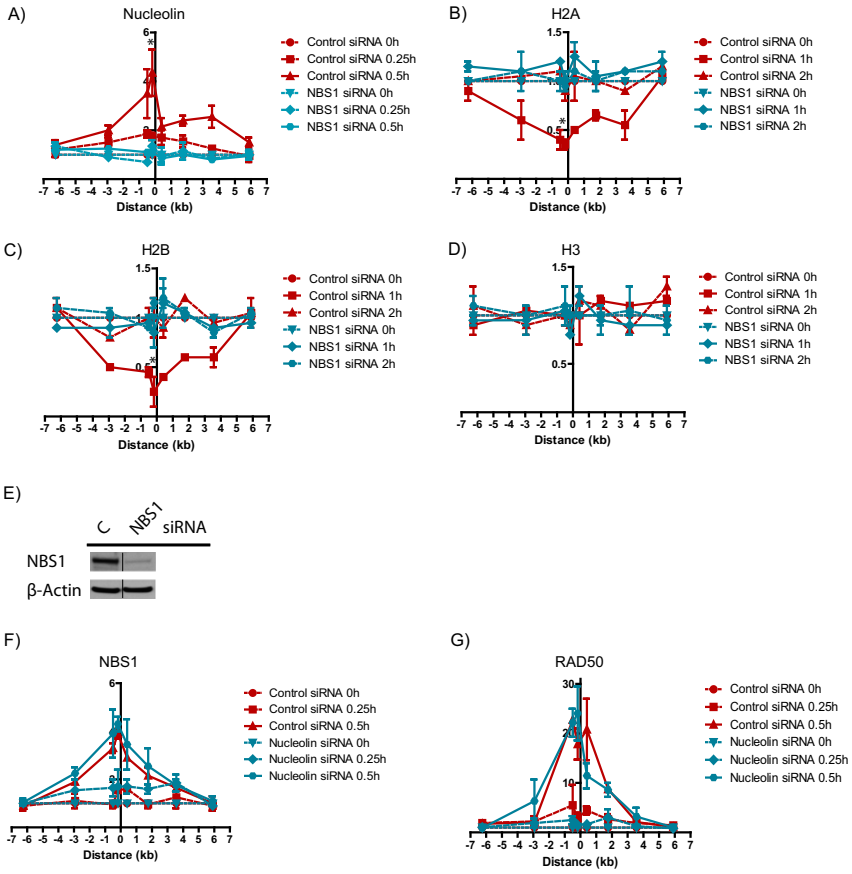

Fig. S6. Nucleolin is recruited to the DSB in an MRE11-NBS1-RAD50 (MRN) complex-dependent manner to facilitate nucleosome disruption. (*A–D*) NBS1 knockdown abrogates nucleolin recruitment to the DSB and nucleosome disruption. ChIP of (*A*) nucleolin, (*B*) histone H2A, (*C*) histone H2B, and (*D*) histone H3 in MCF7 cells stably expressing ddI-PpoI as described in Fig. 1*B* that were cultivated in medium containing 0.1% FBS for 24 h before DSB induction. Cells were transfected with non-targeting control siRNA or NBS1-targeting siRNA. (*E*) Western blot showing down-regulation of NBS1 expression by siRNA. (*F* and *G*) Recruitment of the MRN complex to the DSB is independent of nucleolin. ChIP of (*F*) NBS1 and (*G*) RAD50 in MCF7 cells stably expressing ddI-PpoI as described in Fig. 1*B* that were cultivated in medium containing 0.1% FBS for 24 h before DSB induction. Cells were transfected with nontargeting control siRNA or nucleolin-targeting siRNA. $*P < 0.05$.

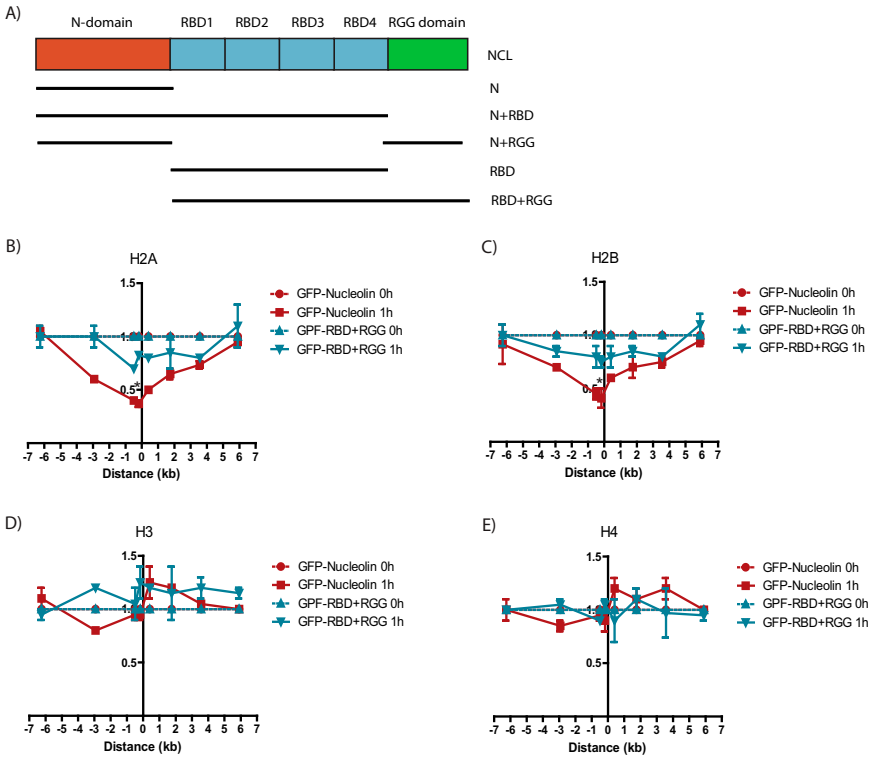

Fig. S7. N-terminal domain of nucleolin is required for nucleosome disruption. (*A*) A schematic diagram displaying the functional domains of nucleolin and nucleolin-deletion mutants that were used in this study. RBD, RNA-binding domain; RGG, arginine- and glycine-rich C-terminal domain. (*B–E*) Overexpression of the N-terminal deletion mutant of nucleolin attenuates nucleosome disruption. ChIP of (*B*) histone H2A, (*C*) histone H2B, (*D*) histone H3, and (*E*) histone H4 in MCF7 cells stably expressing ddI-PpoI as described in Fig. 1*B* that were cultivated in medium containing 0.1% FBS for 24 h before DSB induction. Cells were transiently transfected with full-length nucleolin or the N-terminal nucleolin mutant consisting of the RBD and RGG domains. $*P < 0.05$.

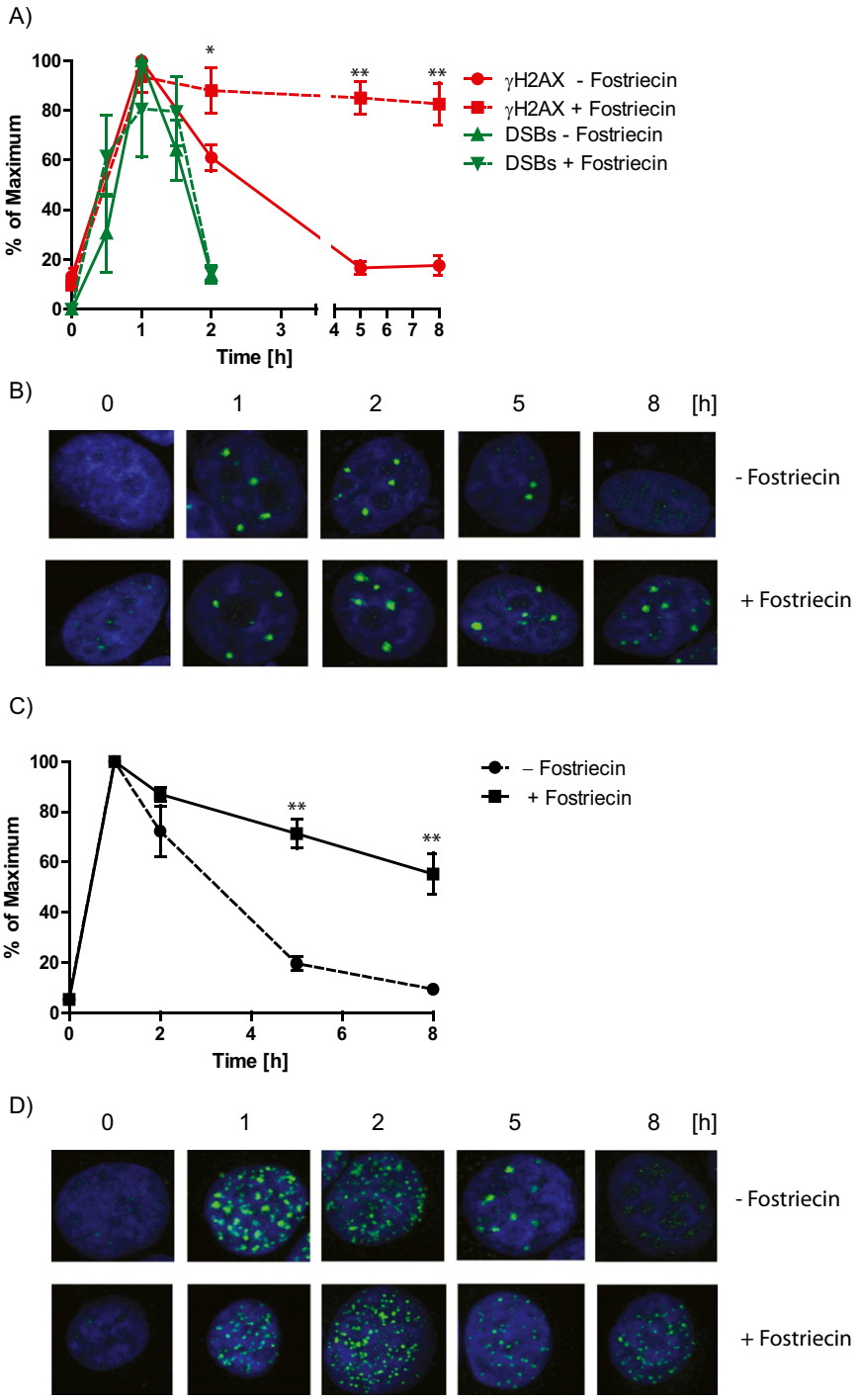

Fig. S8. Phosphatase PP2A inhibition delays γH2AX foci resolution without affecting DSB repair assessed by PCR. (*A*) Quantification of immunostained γH2AX foci following a transient ddI-PpoI induction and DSBs measured by repair assay in MCF7 cells stably expressing ddI-PpoI as described in Fig. 1*A*, normalized to the maximal number of foci per cell and the maximal DNA cleavage, respectively. The phosphatase PP2A inhibitor fostriecin was added 1 h before 4-OHT and was present during treatment and recovery. Time indicated is hours after the addition of 4-OHT. Data are shown as the mean ± SEM of three independent experiments. (*B*) Representative images of the γH2AX foci from A. (*C*) Quantification of immunostained γH2AX foci in MCF7 cells (normalized to the maximal number of foci per cell) following a 1-h pulse treatment with 2 μM etoposide. Fostriecin was added 1 h before etoposide and was present during treatment and recovery. The time indicated is hours after the addition of etoposide. Data are shown as the mean ± SEM of three independent experiments. (*D*) Representative images of γH2AX foci from C. $*P < 0.05$, $**P < 0.01$.

Table S1. Primer sequences for real-time PCR used for ChIP and DSB-repair assays

Description	Sequence	Annealing temperature, °C
Oligos for real-time PCR DSB-repair assay for human cells		
I-PpoI site at chromosome 1 (flanking the I-PpoI site)	5′TCACTGAAGACTTGGTGGGA3′	60.0
	5′AAACCATACGTGGCAGAGTG3′	
GAPDH site	5′GCTTGCCCTGTCCAGTTAAT3′	60.0
	5′TAGCTCAGCTGCACCCTTTA3′	
Oligos for real-time PCR ChIP assay, bp (I-PpoI cut site at 10,000 bp)		
3,753	5′TGCCTAAATGCCTCTTTCTACTG3′	60.0
	5′AAGCTGGAAATTGGCCTAGA3′	
7,073	5′TAAACACTGGGTGCCTTTCA3′	60.0
	5′CCCAAACATACCAACATCCA3′	
9,503	5′CTCCAGGGCATCCTTAGTGT3′	60.0
	5′GGGCCAGGTGTGTACTTAGG3′	
9,818	5′TTCACAGCACTCTCCATTCC3′	60.0
	5′TCTTTCCCACCAAGTCTTCA3′	
10,407	5′TTCCCATTATCTGAAGAGCGT3′	60.0
	5′TGGATGGCTCTGATAGTTACAAA3′	
11,755	5′GGTTGTTCACACCCTTTCTG3′	60.0
	5′CAAGCACAGAGACTCAAATGC3′	
13,563	5′GGCTTGTAACCCACAACACA3′	60.0
	5′GATGCTGCTCATACCCAATG3′	
15,903	5′AGCCTCGTGTCCATTCTCAT3′	60.0
	5′GATGGAGGACAATTATGATGTGA3′	
Oligos for real-time PCR DSB-repair assay for mouse cells		
I-PpoI site at chromosome 3 (flanking the I-PpoI site)	5′TAGGAACCATGTGTGTAAGTTTG3′	60.0
	5′ACGCAACCATTTAGTCATCTTA3′	
GAPDH site	5′TGACAACTTTGGCATTGTGGAAGG3′	60.0
	5′CCATCACGCCACAGCTTTCCAGAG3′	